Cell Reports, Volume *22*

Supplemental Information

Surface-Matrix Screening Identifies Semi-specific Interactions that Improve Potency of a Near Pan-reactive HIV-1-Neutralizing Antibody

Young D. Kwon, Gwo-Yu Chuang, Baoshan Zhang, Robert T. Bailer, Nicole A. Doria-Rose, Tatyana S. Gindin, Bob Lin, Mark K. Louder, Krisha McKee, Sijy O'Dell, Amarendra Pegu, Stephen D. Schmidt, Mangaiarkarasi Asokan, Xuejun Chen, Misook Choe, Ivelin S. Georgiev, Vivian Jin, Marie Pancera, Reda Rawi, Keyun Wang, Rajoshi Chaudhuri, Lisa A. Kueltzo, Slobodanka D. Manceva, John-Paul Todd, Diana G. Scorpio, Mikyung Kim, Ellis L. Reinherz, Kshitij Wagh, Bette M. Korber, Mark Connors, Lawrence Shapiro, John R. Mascola, and Peter D. Kwong

SUPPLEMENTAL INFORMATION

Supplemental Experimental Procedures

Constructs, expression and purification of antibody variants. 298 expression constructs for 10E8 antibody variants were generated with site-directed mutagenesis using 10E8 light or heavy chain expressing pVRC8400 vector as a template. To express variant antibodies, 0.15 ml of Turbo293 transfection reagent (Speed BioSystems) were added to 2.5 ml Opti-MEM medium (Life Technology) and incubated for 5 min at room temperature (RT). Meanwhile, 50 μg of plasmid DNAs (25 μg of heavy chain and 25 μg of light chain) were added to 2.5 ml of Opti-MEM medium in another tube. The 2.5 ml Opti-MEM medium containing 0.15 ml of Turbo293 were then mixed with the 2.5 ml Opti-MEM medium containing 50 μg of plasmid DNAs, incubated for 15 min at RT, and added to 40 ml of Expi293 cells (Life Technology) at 2.5 million cells/ml. The transfected cells were cultured in shaker incubator at 120 rpm, 37 °C, 9% CO_2 overnight. On the second day of transfection, 4 ml of AbBooster medium (ABI scientific) were added to each flask of transfected cells and the flasks were transferred to shaker incubators at 120 rpm, 33 °C, 9% CO_2 for additional 5 days. At 6 days after transfection, supernatants were harvested and purified over 0.5 ml Protein A (GE Health Science) resin in columns. Each antibody was eluted with IgG elution buffer (Pierce), immediately neutralized with one tenth volume of 1M Tris-HCL pH 8.0. The antibodies were then buffer exchanged in PBS by dialysis, adjusted concentration to 0.5 mg/ml and filtered (0.22 μm) for neutralization assays.

Crystallization, structure determination and refinement. 10E8v4-5R+100cF IgG was produced and its antigen-binding fragment (Fab) was generated as described (Kwon et al., 2016). For crystallization, 10E8v4-5R+100cF Fab and gp41 peptide ($_{668}$SLWNWFDITKWLWYIK$_{683}$RRR) were mixed 1:3 molar ratio of protein:gp41 peptide and concentrated to ~10 mg/ml in buffer containing 5 mM HEPES, 7.4, 150 mM NaCl. Then the concentrated protein-gp41 peptide complex was robotically screened for crystallization conditions using Hampton Research, Wizard Screen, and Precipitation Synergy Screen. Initial crystallization conditions were further optimized to grow diffracting quality crystals in hanging drop vapor diffusion where the mixture of 0.5 ul of protein and 0.5 ul of reservoir solution was equilibrated against the reservoir solution containing 12% PEG 3350, 5% iso-propanol, and 0.1M Ammonium Citrate, 7.5. Crystals were cryo-protected by soaking into a solution containing 15% glycerol, 15% ethylene glycol, 7.5% 2r3r-butanediol, 12% PEG 3350, 5% iso-propanol, 0.1M Ammonium Citrate, 7.5 and flash frozen in liquid nitrogen for data collection at synchrotron beamline, SER-CAT ID22, Advanced Photon

Source, Argonne National Laboratory. Diffraction data were processed and scaled using HKL2000 (Otwinowski and Minor, 1997). The structure was solved by molecular replacement using search model, PDB ID 5IQ9, with Phaser (McCoy et al., 2007), built with Coot (Emsley and Cowtan, 2004) and refined with PHENIX (Adams et al., 2010). Crystallographic data and refinement statistics are summarized in table S2.

Binding kinetics by bio-layer interferometry. We used Octet RED 384 (*forté*BIO) to determine the binding kinetics of gp41 MPER peptide-antibody interactions. Streptavidin biosensors were wetted in PBS with 1% BSA for 10 min. Then the biosensors were loaded with biotinylated gp41 peptide (biotin-$_{661}$GELDKWASLWNWFNITNWLWYIK$_{683}$) by immersing into 125 nM of the MPER peptide in PBS with 1% BSA for 5 min. IgGs were prepared in 2-fold dilution series in PBS with 1% BSA starting at 250 nM. Association and dissociation were monitored for 5 min. each. The curves were fitted globally by 1:1 binding model to extract the binding kinetics.

Surface plasmon resonance analysis. BIAcore experiments were carried out using a BIAcore 3000 with the Pioneer L1 sensor chip at 25 °C. The running buffer was 20 mM HEPES containing 0.15 M NaCl, pH 7.4. To measure the relative binding reactivity of bnAbs for MPER embedded in membrane, 40 µl of MPER-halfTM/liposome, consisting of MPER-halfTM (HxB2 sequence a.a 662-693) at a 1:50 molar ratio of peptide to lipids using DOPC and DOPG (4:1) with a liposome concentration of 2 mg/ml, was applied to the L1 chip surface at a flow rate of 5 µl/min. To remove any multi-lamellar structures from the lipid surface, sodium hydroxide (20 µl, 25 mM) was injected at a flow rate of 100 µl/min, which resulted in a stable base line corresponding to the immobilized liposome bilayer membrane with response units of 4500-5000. Antibody solution (10 µg/ml) was then passed over the MPER-halfTM/liposome surface for 3 min at a flow rate of 10µl/min. The immobilized liposomes were completely removed with an injection of 40 mM CHAPS (25 µl) at a flow rate of 5µl/min, followed by a 15 µl injection of NaOH (50 mM)/isopropyl alcohol (6:4) at a 50 µl/min flow rate. Each antibody injection was performed on a freshly prepared liposome surface.

Identification of membrane proximal residues. PDB:5FUU (Lee et al., 2016) with fitted MPER/10E8 was reoriented such that the symmetry axis of the JR-FL EnvdCT trimer is along the z-axis. 10E8v4, 4E10, and DH511.2

were aligned onto the model using their corresponding structures in complex with the MPER. CAP248-2B was aligned onto the model based on aligning a published CAP248-2B/trimer EM model (Wibmer et al., 2017). For these four antibodies, residues with at least one heavy atom within five angstroms along the z axis from the C alpha atom of residue 684 were considered as membrane proximal residues. The membrane proximal residues for 2F5 were inferred from prior study of Ofek et al. (Ofek et al., 2004).

Polyreactivity characterization. Antibodies were assessed for auto-reactivity on two platforms: anti-nuclear antibodies by staining on HEp2 cells (ZEUS Scientific Cat. No: FA2400, ANA HEp2 Test System) and anti-cardiolipin ELISA (Inova Diagnostics Cat. No: 708625, QUANTA LITE ACA IgG III) as per the manufacturer's instructions. On HEp2 cells, antibodies were tested at 50 and 25 µg/ml. Control antibodies VRC01-LS, 4E10 and VRC07-G54W were included in each slide and assigned a score between 0 and 3+. Test antibodies scored greater than 1+ at 25 µg/ml were considered autoreactive. In the cardiolipin binding assay, monoclonal antibodies scored greater than three times background at 33 µg/ml were considered autoreactive.

Manufacturing characteristics of 10E8 variants

Appearance evaluation. Test samples were visually inspected to assess the color and clarity by examining against both black and white background under fluorescent lighting using a Bosch MIH-DX Manual Visual Inspection Hood. Each vial was gently swirled prior to examination to re-suspend settled particles. Appearance parameters evaluated included color, turbidity, opalescence, visible particle size and frequency.

Concentration determination by UV-Visible spectroscopy. UV-visible spectra were acquired using a single-beam diode array spectrophotometer (Agilent 8453, GE Healthcare) in a 10 mm path length quartz cuvette with a 180 µl useable sample volume. The instrument was blanked with the appropriate buffers and sample data was collected from 200 – 600 nm, with 1 nm data intervals and 0.5 second integration. Optical density was quantified using the signal at 350 nm. Reported absorbance results were light scattering corrected using ChemStation software, calculated in a non-absorbing range (350-500 nm).

Dynamic light scattering. Hydrodynamic radii (Rh) and population size distributions (%Pd) were measured by dynamic light scattering (DLS) using the Wyatt DynaPro Plate Reader and Plate Reader II. Samples were analyzed in a Corning™ 384-well plate (30 µl/well, in two 15 µl aliquots for increased accuracy). Six (6) wells were analyzed per sample (three wells per replicate). Data were acquired at 25 ± 2°C for 10 readings per well, at 10 second per acquisition, reporting particles with an Rh in the range of 2 – 2000 nm. Data were fitted to a correlation function algorithm and the regularization fit hydrodynamic radius and population distribution data were generated using the Dynamics software (Wyatt, version 7.1.7).

Thermal transitions by dynamic light scattering. Thermal ramp dynamic light scattering was performed using the Wyatt DynaPro Plate Reader and Wyatt DynaPro Plate Reader II. Thermal transitions analyses were conducted using a centroid plate arrangement; samples were arrayed (n = 2 per replicate) in a solid rectangle in the center of the plate (30 µl/well, in two 15 µl aliquots for increased accuracy). Additionally, the wells surrounding the samples were filled with high-purity paraffin oil to minimize edge effects and an additional 10 µl of paraffin oil was gently layered on top of the sample-containing wells to minimize evaporation. Data were acquired for 5 readings per well, at 5 seconds per acquisition while the temperature was ramped from 25°C to 70°C at a rate of 0.12°C / minute. Particle data was reported for Rh values in the range of 2 – 5000 nm.

The thermal transition onset (Tonset) for each sample was determined using the onset function (50 – 60°C range with no zero-slope parameter applied) in Dynamics version 7.1.9. Outlying data points and data points for which gross aggregation had occurred (Rh > ~500 nm) were marked until the line of fit overlaid suitably with the remaining data points, as viewed from a y-axis (cumulative Rh) scale of 0 – 150 nm. As transient fluctuations in signal due to aggregation are indistinguishable from contaminant (dust) particle interference, no further data screen was applied.

Differential scanning calorimetry. Differential scanning calorimetry (DSC) analysis was performed using a GE Healthcare VP-Capillary differential scanning calorimeter (DSC). Samples were heated from 10 – 90°C at a rate of 1°C/minute (no reverse scans were acquired). Data were analyzed using MicroCal Origin (version 7.0) and were subjected to buffer subtraction and baseline correction prior to determination of thermal transition midpoints (Tm).

Circular dichroism. Far UV circular dichroism spectroscopy was performed using a Chirascan-plus Circular Dichroism Spectrometer (Applied Photophysics Ltd) equipped with a Peltier temperature controller and a 6-position cuvette holder. Spectra were collected from 195-260 nm for initial scans using a 0.1 cm path length cuvette. Baseline measurement of the buffer was taken and subtracted from sample measurements prior to data analysis.

Isothermal chemical denaturation. Isothermal chemical denaturation experiments were carried out using ICD 2304 Isothermal Chemical Denaturation System (Unchained Labs) equipped with a fluorescence detector. The stability of the monoclonal antibodies in a pH range of 4.5 - 7.0 and NaCl concentration range of 0 - 200 mM was determined by denaturing the samples in a linear gradient of urea from 0 to 9 M. A buffer system of 10 mM sodium phosphate, sodium succinate, and histidine was used to generate the pH range. All dilutions for the pH range, NaCl and urea concentration was performed by the instrument. The denaturation of the antibodies was detected by monitoring the intrinsic fluorescence using an excitation wavelength of 280 nm and recording the emission spectra between 300 - 500 nm. Data processing was performed with the software provided by the instrument to identify the denaturation midpoint (C1/2).

Ultrafiltration. Ultrafiltration was performed using an Amicon Stirred cell concentrator Model:8003 (EMD Millipore) using a 30 kD Ultracel regenerated cellulose filter discs to increase the concentration of the antibodies. Nitrogen gas pressure of ~ 60 psi was applied and the protein solution was stirred constantly to prevent the formation of a concentration gradient. The concentration of the antibody in the cell was monitored over approximately 6 hours by UV-visible spectroscopy as described above.

Antibody half-life in rhesus macaque. Male *Macaca mulatta* animals of Indian origin were used in these studies. All animal experiments were reviewed and approved by the Animal Care and Use Committee of the Vaccine Research Center, NIAID, NIH, and all animals were housed and cared for in accordance with local, state, federal, and institute policies in an American Association for Accreditation of Laboratory Animal Care (AAALAC)-accredited facility at the NIH. Indian rhesus macaques were infused intravenously with 10 mg/kg of monoclonal antibody. Endotoxin levels were measured for each antibody preparation by the QCL-1000™ endpoint chromogenic LAL assay (Lonza) and were all below 0.5 EU/mg levels. Whole blood samples were collected prior to

injection, and at time points 0, 30 mins, 6 hours, 12 hours, and days 1, 2, 4, 7, and 14. Plasma was separated by centrifugation. Plasma samples were heat-inactivated at 56°C for 30 minutes, and lipoproteins were pelleted. Plasma antibody levels were determined by ELISA.

SUPPLEMENTAL REFERENCES

Adams, P.D., Afonine, P.V., Bunkoczi, G., Chen, V.B., Davis, I.W., Echols, N., Headd, J.J., Hung, L.W., Kapral, G.J., Grosse-Kunstleve, R.W., *et al.* (2010). PHENIX: a comprehensive Python-based system for macromolecular structure solution. Acta Crystallogr D Biol Crystallogr *66*, 213-221.

Emsley, P., and Cowtan, K. (2004). Coot: model-building tools for molecular graphics. Acta Crystallogr D Biol Crystallogr *60*, 2126-2132.

Kwon, Y.D., Georgiev, I.S., Ofek, G., Zhang, B., Asokan, M., Bailer, R.T., Bao, A., Caruso, W., Chen, X., Choe, M., *et al.* (2016). Optimization of the Solubility of HIV-1-Neutralizing Antibody 10E8 through Somatic Variation and Structure-Based Design. J Virol *90*, 5899-5914.

Lee, J.H., Ozorowski, G., and Ward, A.B. (2016). Cryo-EM structure of a native, fully glycosylated, cleaved HIV-1 envelope trimer. Science *351*, 1043-1048.

McCoy, A.J., Grosse-Kunstleve, R.W., Adams, P.D., Winn, M.D., Storoni, L.C., and Read, R.J. (2007). Phaser crystallographic software. J Appl Crystallogr *40*, 658-674.

Ofek, G., Tang, M., Sambor, A., Katinger, H., Mascola, J.R., Wyatt, R., and Kwong, P.D. (2004). Structure and mechanistic analysis of the anti-human immunodeficiency virus type 1 antibody 2F5 in complex with its gp41 epitope. J Virol *78*, 10724-10737.

Otwinowski, Z., and Minor, W. (1997). Processing of X-ray diffraction data collected in oscillation mode. Methods Enzymol *276*, 307-326.

Wibmer, C.K., Gorman, J., Ozorowski, G., Bhiman, J.N., Sheward, D.J., Elliott, D.H., Rouelle, J., Smira, A., Joyce, M.G., Ndabambi, N., *et al.* (2017). Structure and Recognition of a Novel HIV-1 gp120-gp41 Interface Antibody that Caused MPER Exposure through Viral Escape. PLoS Pathog *13*, e1006074.

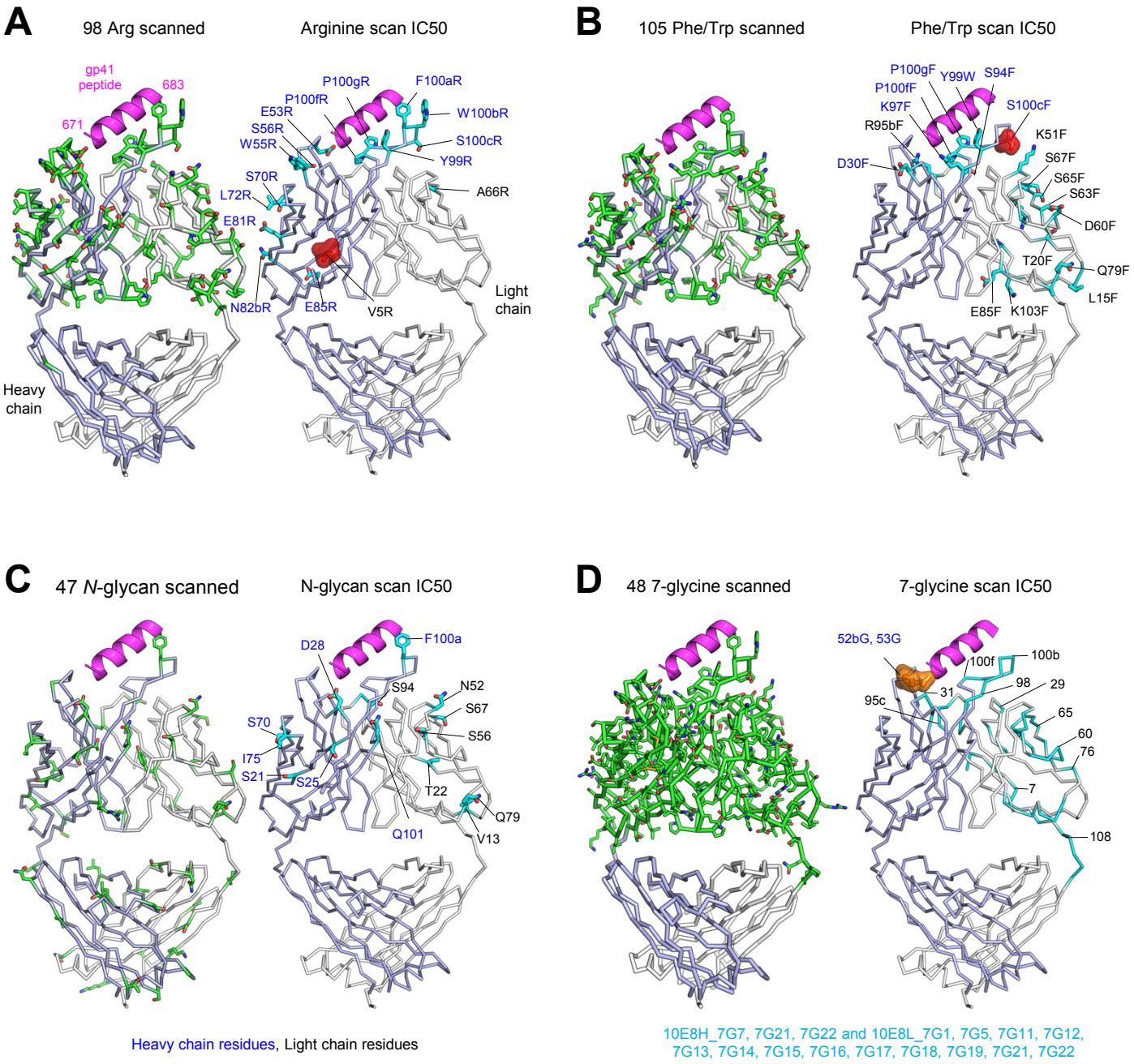

Figure S1. Surface matrix-screening of antibody 10E8 with neutralization readout. Related to Figures 1 and 2. (**A**) 98 10E8 heavy chain (light blue) and light chain (white) residues screened with Arginine for improved potency were shown in stick representation (left) and colored as defined in figure key. (**B**) 105 10E8 heavy and light chain residues screened with Phe/Trp for improved potency were shown in stick representation (left). Phe/Trp variants were shown in the same color scheme as in (A) (right). (**C**) 47 10E8 heavy and light chain residues that were mutated to add an N-linked glycan were shown in stick representation (left). N-linked glycan variants were shown in the same color scheme as in (A) (right). (**D**) 10E8 heavy and light chain residues that were part of 48 7-glycine substituted variants were shown in stick representation (left). Positions which are part of 7-glycine substituted variants were highlighted as in (A) (right). 7-glycine substituted variants with the potency impaired greater than 3.41-fold were listed. See the sequences of the variants in Table S1.

A

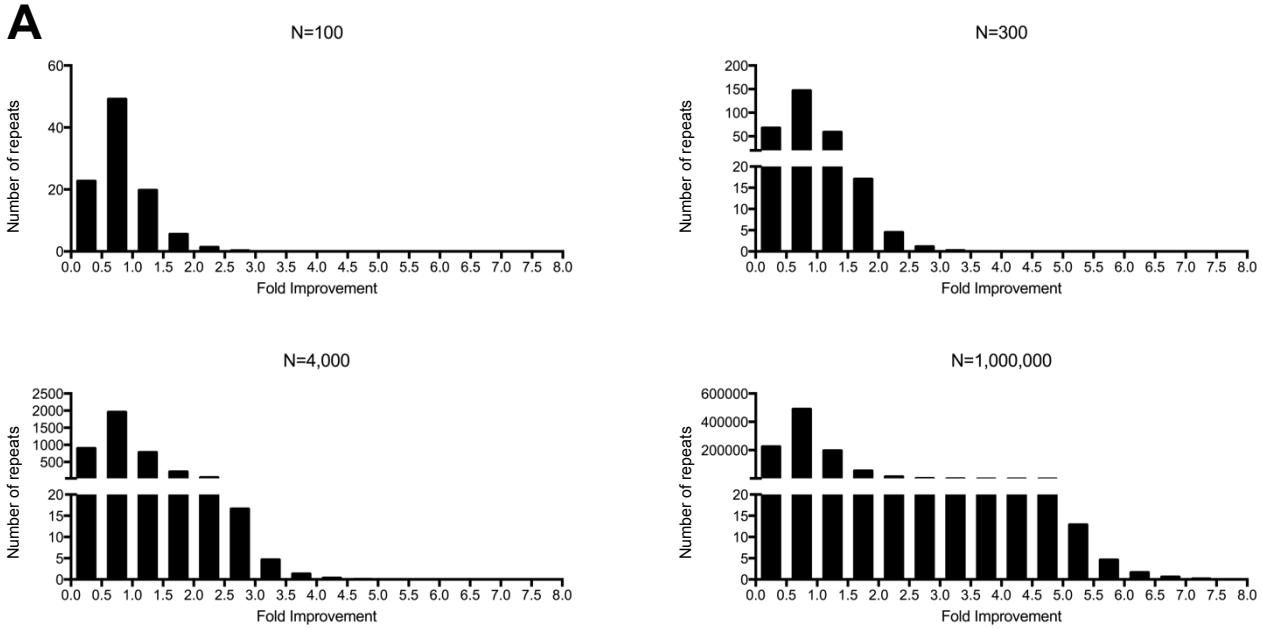

B

	N=100	N=300	N=4000	N=1000000
Fold improvement for top 10	2.84	3.29	4.41	7.27
	2.41	2.84	3.92	6.64
	2.21	2.64	3.7	6.37
	2.08	2.51	3.56	6.18
	1.99	2.41	3.45	6.05
	1.91	2.33	3.37	5.95
	1.85	2.27	3.3	5.86
	1.79	2.21	3.24	5.78
	1.74	2.17	3.19	5.72
	1.7	2.12	3.14	5.66

Figure S2. Minimum observable signal, as a function number of variants screened with an assay variability σ_g of 1.5. Related to Figures 1 and 2. (**A**) Theoretical distribution of fold improvement observed when the same measurement is repeated N times, assuming a log-normal distribution. (**B**) Top ten fold improvement observed when the same measurement is repeated N times.

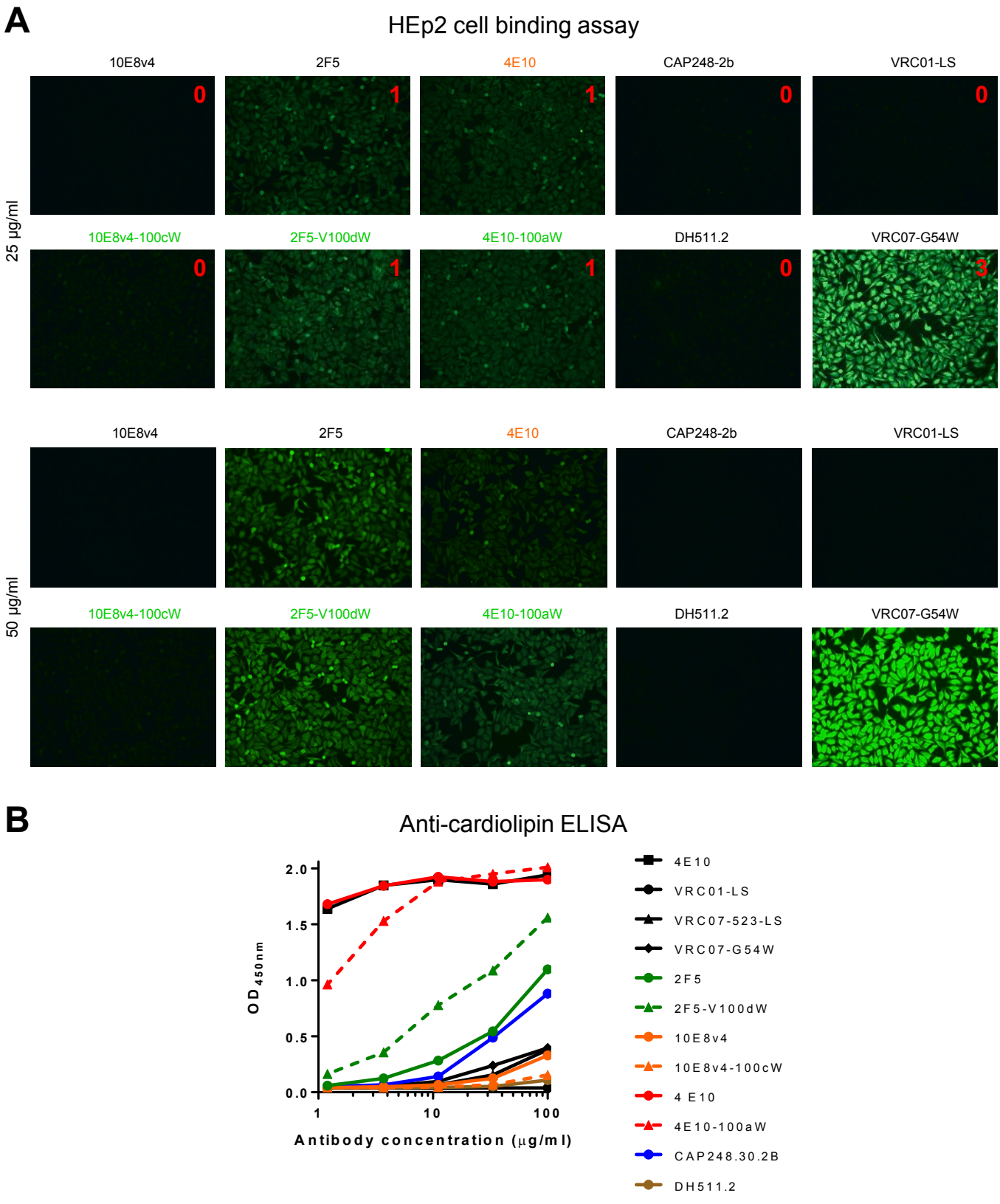

Figure S3. Polyreactivity of 10E8 antibody variants and other MPER-directed antibodies with hydrophobic substitutions. Related to Figure 5. (**A**) In the HEp2 cell staining assay, antibodies were tested at 25 and 50 µg/ml with control antibodies, VRC01-LS, 4E10 and VRC07-G54W. Control antibodies were assigned a score between 0 and 3+. Test antibodies scored greater than 1+ at 25 µg/ml were considered autoreactive. (**B**) Cardiolipin binding assay. Antibodies scored three times greater than background at 33 µg/ml were considered autoreactive.

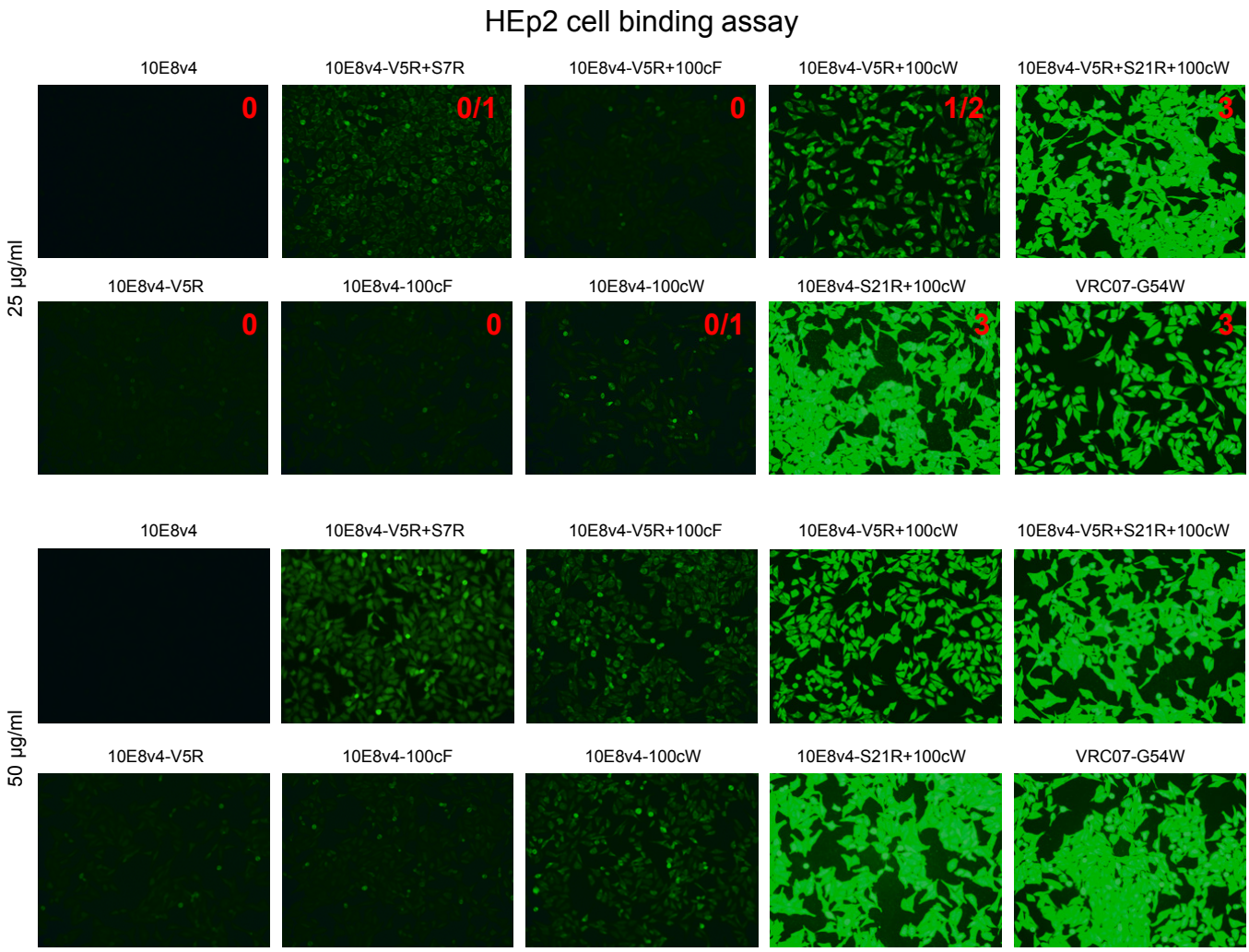

Figure S4. Polyreactivity of 10E8 antibody variants with positively charged substitutions. Related to Figure 6. With HEp2 cell staining assay, antibodies were tested at 25 and 50 µg/ml along with control antibodies, VRC01-LS, 4E10 (shown in Figure S3) and VRC07-G54W. Control antibodies were assigned a score between 0 and 3+. Test antibodies scored greater than 1+ at 25 µg/ml were considered autoreactive.

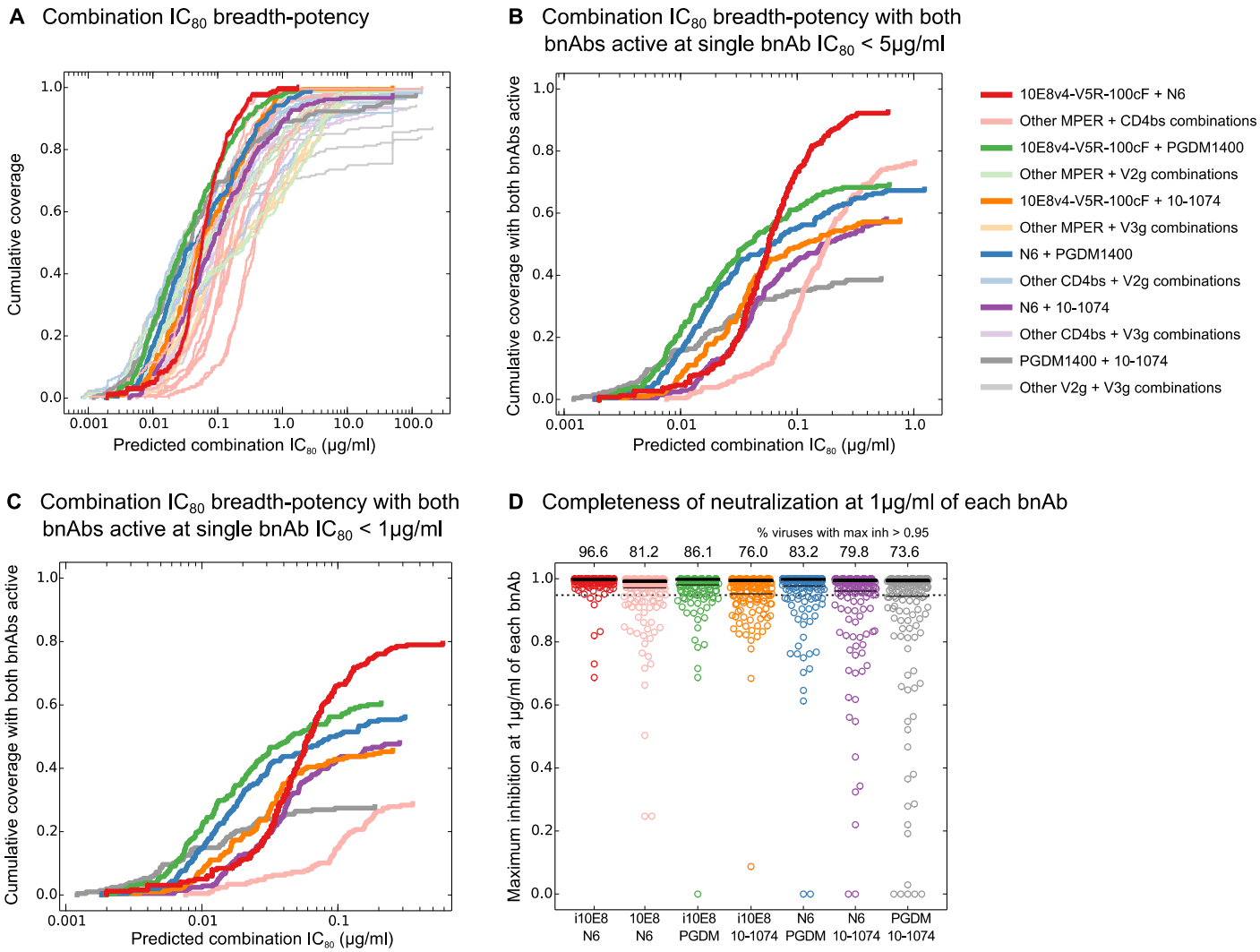

Figure S5. Predicted neutralization for antibody combinations, including those with 10E8v4-5R+100cF. Related to Figure 7. (**A**) IC_{80} breadth potency curve for 2 bnAb combinations. Each combination is assumed to have equal concentrations of each bnAb and combination IC_{80} is the concentration of each bnAb for 80% neutralization of a given virus. Bold, dark lines show data for the best-in-class combinations, and thin, faint lines show data for other combinations from the same class. Experimental IC_{80} data is shown for the combination of 10E8v4-5R+100cF with N6. (**B**) IC_{80} breadth-potency curves with both bnAbs active at single bnAb IC_{80} < 5 µg/ml. The cumulative coverage is plotted versus combination IC_{80} considering only those viruses neutralized by both bnAbs. A virus was considered neutralized by a bnAb if individual bnAb IC_{80} < 5 µg/ml. The pink curve shows coverage with both bnAbs active for 10E8 + N6. Experimental IC_{80} data is shown for the combination of 10E8v4-5R+100cF with N6. (**C**) Same as B using activity threshold of single bnAb IC_{80} < 1 µg/ml. (**D**) Predicted completeness of neutralization for antibody combinations at 1µg/ml of each bnAb. The numbers on top indicate the percent viruses that were predicted to be neutralized at >95%.

Table S2. Crystallographic data and refinement. Related to Figure 1.

	10E8v4-5R+100cF Fab:gp41 peptide
PDB accession code	5WDF
Data collection	
Space group	*P*1
Cell constants	
a, *b*, *c* (Å)	57.2 60.9, 70.1
α, β, γ (°)	103.0, 107.4, 100.0
Unique reflections	14,534
Wavelength (Å)	1.00
Resolution (Å)	50.0-3.1 (3.15-3.10)*
R_{merge}	11.1 (48.4)
R_{pim}	7.9 (36.7)
$CC_{1/2}$	0.915 (0.715)
$I / \sigma I$	11.0 (2.1)
Completeness (%)	93.2 (83.6)
Redundancy	2.6 (2.0)
Refinement	
Resolution (Å)	45.1-3.1
Reflections used in refinement	14,394
R_{work} / R_{free} (%)	24.6/28.1
No. atoms	
Protein	6,558
B-factors (Å^2)	
Protein	114
R.m.s. deviations	
Bond lengths (Å)	0.002
Bond angles (°)	0.605
Ramachandran	
Favored regions (%)	95.3
Allowed regions (%)	4.42
Disallowed regions (%)	0.25

* Values in parentheses are for highest-resolution shell.